HHS Public Access

Author manuscript

Cell Stem Cell. Author manuscript; available in PMC 2018 December 07.

Published in final edited form as:

Cell Stem Cell. 2017 December 07; 21(6): 806–818.e5. doi:10.1016/j.stem.2017.11.008.

mTORC1 activation during repeated regeneration impairs somatic stem cell maintenance

Samantha Haller[1,8], **Subir Kapuria**[1], **Rebeccah R. Riley**[1], **Monique N. O'Leary**[1,2], **Katherine H. Schreiber**[1,3], **Julie K. Andersen**[1], **Simon Melov**[1], **Jianwen Que**[4], **Thomas A. Rando**[6], **Jason Rock**[5], **Brian K. Kennedy**[1], **Joseph T. Rodgers**[6,7], and **Heinrich Jasper**[1,8,9,*]

[1]Buck Institute for Research on Aging, 8001 Redwood Boulevard, Novato, CA 94945-1400, USA

[2]Mount Holyoke College, South Hadley, MA 01075, USA

[3]University of Michigan, Ann Arbor, MI 48109, USA

[4]Department of Medicine, Columbia University, New York, NY 10032, USA

[5]Department of Anatomy, UCSF School of Medicine, San Francisco, CA 94117, USA

[6]Paul F. Glenn Laboratories for the Biology of Aging; Stanford University School of Medicine; Stanford, CA 94304, USA

[7]Eli and Edythe Broad CIRM Center for Regenerative Medicine and Stem Cell Research, USC, Los Angeles, CA 90033, USA

[8]Immunology Discovery, Genentech, Inc., 1 DNA Way, South San Francisco, CA 94080, USA

[9]Leibniz Institute on Aging - Fritz Lipmann Institute, Jena, 07745, Germany

Summary

The balance between self-renewal and differentiation ensures long-term maintenance of stem cell (SC) pools in regenerating epithelial tissues. This balance is challenged during periods of high regenerative pressure and is often compromised in aged animals. Here we show that TOR signaling is a key regulator of SC loss during repeated regenerative episodes. In response to regenerative stimuli, SCs in the intestinal epithelium of the fly and in the tracheal epithelium of mice exhibit transient activation of TOR signaling. Although this activation is required for SCs to rapidly proliferate in response to damage, repeated rounds of damage lead to SC loss. Consistently, age-related SC loss in the mouse trachea and in muscle can be prevented by pharmacologic or genetic inhibition of mTORC1 signaling, respectively. These findings highlight

*Lead Contact; correspondence to: jasperh@gene.com, Phone: (650) 797 7040.

Author Contributions

Conceptualization, S.H., S.K., J.T.R., T.A.R., B.K.K. and H.J.; Methodology, S.H., S.K., R.R., J.T.R., J.Q., T.A.R., B.K.K. and H.J.; Investigation, S.H., S.K., R.R., J.T.R; Writing – Original Draft, S.H., J.T.R. and H.J.; Writing – Review & Editing, S.H., J.T.R., R.R., S.K., J.Q., J.R., B.K.K. and H.J.; Funding Acquisition, J.Q., J.R., B.K.K. and H.J.; Resources, M.N.O., K.H.S., J.K.A., S.M., J.R. and B.K.K.; Supervision, T.A.R. and H.J.

an evolutionarily conserved role of TOR signaling in SC function and identify repeated rounds of mTORC1 activation as a driver of age-related SC decline.

eTOC blurb

Studying flies and mice, Jasper and colleagues demonstrate that repeated regenerative episodes results in the loss of tissue stem cells (SCs) due to the transient activation of the growth regulator mTORC1 during SC activation. Pharmacological inhibition of mTORC1 can prevent this loss and limit the age-related decline in SC numbers.

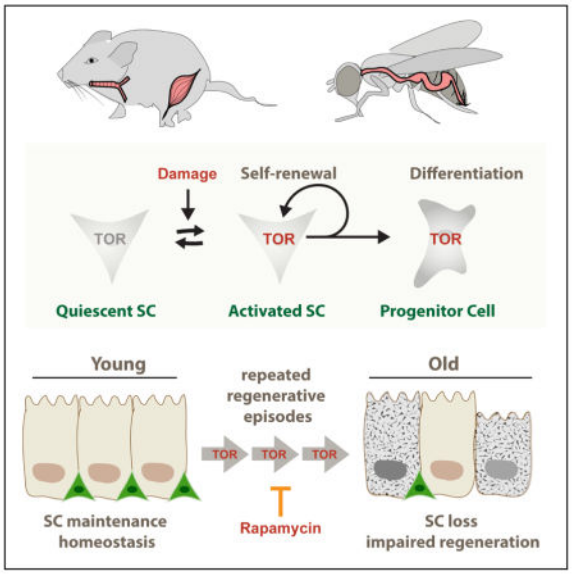

Introduction

Regenerative processes in somatic tissues require coordinated regulation of stem cell proliferation and daughter cell differentiation to ensure long-term tissue homeostasis (Chandel et al., 2016; Jones and Rando, 2011). Studies in a wide range of model systems indicate that the loss of this coordination contributes to regenerative dysfunction in aging tissues. Understanding the causes and consequences of age-related dysregulation of these processes is likely to identify intervention strategies to maintain stem cell function and improve regenerative capacity in aging tissues.

Barrier epithelia are exposed to frequent environmental challenges, and are thus under repeated regenerative pressure during the lifespan of an organism. Accordingly, age-related stem cell dysfunction is particularly evident in barrier epithelia of aging organisms, resulting in dysplasias, degenerative diseases, and cancers (Li and Jasper, 2016; Wansleeben et al., 2014). The *Drosophila* posterior midgut epithelium has emerged as an excellent model system to study the causes and consequences of age-related regenerative dysfunction of barrier epithelia (Ayyaz and Jasper, 2013). Excessive proliferation and mis-differentiation of intestinal stem cells (ISCs) is a common phenotype in aging flies, resulting in epithelial dysplasia and the breakdown of the epithelial barrier function. These phenotypes contribute

to mortality in old flies, and interventions that limit and delay their progression frequently result in lifespan extension (Guo et al., 2014; Li et al., 2016; Wang et al., 2015).

In young animals, ISCs divide infrequently under homeostatic conditions, but are rapidly and transiently activated in response to damage to the intestinal epithelium (Ayyaz et al., 2015; Biteau et al., 2008; Jiang et al., 2009). During such regenerative episodes, ISCs divide to self-renew and produce enteroblasts (EB), which undergo differentiation to become either enterocytes (ECs) or enteroendocrine cells (EEs) (Ayyaz and Jasper, 2013; Li et al., 2016). To adjust proliferative responses to changing local, systemic, and environmental conditions, ISCs integrate a wide range of growth factor, inflammatory, and stress signals by modulating intracellular calcium levels (Ayyaz and Jasper, 2013; Biteau et al., 2011; Deng et al., 2015a; Li et al., 2016). Differentiation in the ISC lineage is controlled by Delta/Notch (Dl/N) signaling (Ayyaz and Jasper, 2013; Li et al., 2016). Dl is expressed in ISCs and triggers N activation in EBs. In these cells, N coordinates cell specification with cell growth and proliferation by activating the TOR signaling pathway (Kapuria et al., 2012).

As a constituent of the mTORC1 complex, TOR kinase is part of an evolutionarily conserved nutrient sensing pathway that coordinates cellular responses to nutrients by promoting anabolic functions, including translation, and by inhibiting catabolic processes like autophagy (Laplante and Sabatini, 2012). Accordingly, it has a major impact on cell growth, and is among the best understood regulators of tissue and organ size in metazoans (Laplante and Sabatini, 2012). Its repression extends lifespan in different organisms, including flies and mice (Kennedy and Lamming, 2016). mTORC1 can be activated by multiple mechanisms, including by growth factors through Akt-mediated phosphorylation of Tuberous Sclerosis Complex 2 (TSC2; encoded by the gene *gigas* in *Drosophila*) and subsequent inhibition of the TSC1/2 complex (Laplante and Sabatini, 2012). TSC1 promotes the stability of TSC2, a GTPase activating protein for the small GTPase Rheb, inhibiting Rheb-mediated mTORC1 activation. Active mTORC1 phosphorylates translational regulators (including ribosomal protein S6 Kinase, S6K, and eIF4E Binding Protein, 4EBP), autophagy regulators (including ATG1/ULK1), and TFEB transcription factors, resulting in a net increase of protein production, and a decrease in autophagy and lysosome biogenesis (Laplante and Sabatini, 2012, 2013).

Results from (1) fly germline and intestinal stem cell lineages, (2) mouse embryonic, hematopoietic, follicle, muscle and neuronal SCs, (3) induced pluripotent stem cells, and (4) human embryonic SCs suggest that TSC/mTORC1 signaling has an important regulatory role in stem cell maintenance and differentiation (Chen et al., 2011; Magri et al., 2011). In mouse hematopoietic SCs (HSCs), the expression of constitutively active AKT leads to mTORC1-dependent SC loss (Kharas et al., 2010). Loss of *Pten* in HSCs or myogenic progenitors leads to constitutively active AKT and mTORC1 signaling and SC activation that is associated with long-term SC loss (Yilmaz et al., 2006; Yue et al., 2016; Zhang et al., 2006). Sustained activation of mTORC1 in hair follicle SCs (through the activation of Wnt signaling) leads to SC exhaustion (Castilho et al., 2009). In human embryonic stem cells, activation of S6K by mTORC1 has been reported to induce differentiation (Easley et al., 2010), and reduction of mTORC1 activity in Paneth cells (ISC support cells) under dietary restriction promotes ISC maintenance and proliferation through a non-autonomous

mechanism (Yilmaz et al., 2012). mTORC1 also appears to play a critical role in the activation of SC proliferation during regenerative episodes in various systems: short term induction of AKT promotes HSC pool expansion (Kharas et al., 2010), while in a mouse model of muscle injury, mTORC1 activation is necessary to allow rapid proliferation of muscle SCs (MuSCs) by promoting a switch from the G_0 to a mTORC1-dependent 'G_{alert}' state (Rodgers et al., 2014). During hair regeneration, mTORC1 signaling promotes hair follicle SC activation by repressing BMP signaling (Deng et al., 2015b).

In flies, TSC/TOR signaling regulates proliferation and maintenance of SCs according to nutritional conditions both in the germline and the intestine (Amcheslavsky et al., 2011; Hsu and Drummond-Barbosa, 2009; Jasper and Jones, 2010; Kapuria et al., 2012; LaFever and Drummond-Barbosa, 2005; LaFever et al., 2010; McLeod et al., 2010; O'Brien et al., 2011; Quan et al., 2013; Sun et al., 2010). In quiescent ISCs, TOR is repressed by high levels of TSC2. The activation of N in EBs results in the repression of TSC2 expression and subsequent activation of TOR, which is sufficient and required for growth and differentiation of these cells into ECs (Kapuria et al., 2012). TSC/TOR signaling thus serves as a critical determinant of cell identity in the ISC lineage, and repression of TOR by TSC1/2 is required to prevent ectopic ISC differentiation (Amcheslavsky et al., 2011; Kapuria et al., 2012; Quan et al., 2013).

The conflicting requirement for mTORC1 activation to trigger proliferative activity in a wide variety of SCs in flies and mice, and for mTORC1 repression in the long-term maintenance of SCs in these animals, suggests that precise mTORC1 regulation is essential if long-term tissue homeostasis and regenerative capacity is to be preserved. Here, we have asked how the repeated activation of mTORC1 during regenerative episodes impacts long-term maintenance of SCs in the fly intestine and in the mouse tracheal epithelium, two barrier epithelia with similar morphology and regenerative processes. The mouse airway epithelia contain a SC population, the basal cells (BC), which differentiate into either ciliated or secretory cells (Rock et al., 2009). BCs are characterized by expression of Keratin 5 (Krt5) and the transcription factor p63 (Trp63). After injury, BCs rapidly segregate into two populations, expressing either the intracellular domain of Notch2 (N2ICD) or c-myb that commit these cells to the secretory (N2ICD expressing BCs) or ciliated (c-myb expressing BCs) cell lineages (Pardo-Saganta et al., 2015). Activated BCs express both Krt5 and the differentiation marker Keratin 8 (Krt8), transitioning through a so-called Basal Luminal Progenitor (BLP) state, before becoming Early Precursor cells (EPs) which express only Krt8, but no markers of fully differentiated cells (Scgb1a1, Muc5ac, Foxj1, CCSP, AcTub). Secretory cells still have the ability to self-renew and produce ciliated cells (Rock et al., 2011; Watson et al., 2015) and can also dedifferentiate into BCs (Tata et al., 2013). The regulation of BC proliferation closely resembles that of *Drosophila* ISCs (Biteau et al., 2011; Rock et al., 2011). Similar to ISCs, BC differentiation is controlled by Notch activity (Biteau et al., 2011; Rock et al., 2011).

Our study shows that in both systems, mTORC1 is transiently activated in SCs after a regenerative stimulus. The induction of repeated regenerative episodes results in mTORC1-dependent loss of ISCs and BCs, while chronic activation of mTORC1 (by loss of TSC1) causes loss of ISCs or BCs, respectively. Critically, mTORC1 activation is a likely cause of

BC loss in aging mice, as long-term treatment with the mTORC1 inhibitor Rapamycin is sufficient to prevent BC loss and restore BC numbers in aging mice. Our data indicate that this loss may be caused by mTORC1-dependent differentiation of BCs. These effects are conserved in the muscle, as activation of mTORC1 promotes reprogramming of the MuSC transcriptome towards a differentiation signature, and the age-dependent loss of MuSCs can be prevented by limiting mTORC1 activity genetically in these cells. Our findings highlight the evolutionarily conserved role of mTORC1 in coordinating SC proliferation and differentiation, and demonstrate the usefulness of mTORC1 suppressing interventions in promoting regenerative homeostasis of various organ systems.

Results

In homeostatic conditions, TOR signaling is specifically active in EBs of the *Drosophila* intestine, and has to be suppressed in ISCs to prevent their differentiation (Fig. 1A, (Kapuria et al., 2012). At the same time, we observed previously that TOR is essential for normal proliferative activity, as ISCs homozygous for TOR loss of function alleles fail to generate clonal lineages that grow as fast as lineages from wild-type ISCs (Kapuria et al., 2012). A possible explanation for this paradox is that TOR becomes transiently activated in active ISCs. To test this idea, we performed infection studies using *Erwinia Carotovora Carotovora* (*Ecc15*), a mild enteropathogen that induces a synchronized and transient proliferative response in the epithelium (as measured by the increase in mitotic, phospho-histone H3 expressing ISCs; Fig. 1B). Using phosphorylated 4EBP as a readout for TOR activity, we confirmed that TOR is inactive in ISCs under homeostatic conditions (Fig. 1C & C′), but also found that TOR activity increases within 4 hours after *Ecc15* treatment. The p-4EBP antibody reliably detects changes in TOR signaling activity (Kapuria et al., 2012; LaFever et al., 2010; Penney et al., 2012; Cheng et al., 2011; Vachias et al., 2014). ISCs were labeled by YFP expressed under the control of the ISC/EB driver esg::Gal4, combined with the heat-sensitive Gal4 inhibitor $Gal80^{ts}$ and with Gal80 expressed under the control of the Su(H)Gbe promoter to inhibit UAS-linked transgene expression in EBs (McGuire et al., 2003; Micchelli and Perrimon, 2006; Ohlstein and Spradling, 2006; Wang et al., 2014).

The increase in p-4EBP in ISCs depends on TSC/TOR signaling, as over-expression of TSC1 and 2 was sufficient to prevent 4EBP phosphorylation in ISCs, and as knocking down TSC1 results in significantly elevated p-4EBP levels (Fig. 1C′). Consistently, ISC size increases transiently during the regenerative response, and this increase depends on TSC/TOR signaling (Fig. 1D). The ISC phenotypes observed under homeostatic conditions when TSC1 is knocked down suggest that ISCs may also receive signals that activate TOR transiently during homeostatic renewal of the epithelium.

These observations support the notion that TOR activity is induced in ISCs that are under regenerative pressure. To test whether this activation of TOR would be required for normal regeneration in the gut, we knocked-down the TORC1 component dRaptor in ISCs and quantified the number of mitotic ISCs at two timepoints after the challenge. Strikingly, ISC proliferation was significantly lower in raptor-deficient animals in the early phase of the regenerative response, but was higher than in wild-type animals in the recovery phase, suggesting that the induction of ISC proliferation is not inhibited, but delayed in TOR loss-

of-function conditions (Fig. 1B). Together, these results indicate that TOR activation in ISCs is required for the rapid activation of ISC proliferation in response to a challenge. This observation is reminiscent of the role of mTORC1 activation in the regenerative response of mouse satellite cells during muscle regeneration (Rodgers et al., 2014). We cannot exclude, however, that the function of TOR in fly ISCs changes from pro-proliferative in the early phase of the response to anti-proliferative in the late response.

Since activation of TOR in ISCs also promotes their differentiation into ECs (Kapuria et al., 2012), we hypothesized that its repeated activation as part of multiple regenerative episodes could contribute to stem cell exhaustion by triggering spontaneous differentiation. We tested this hypothesis by performing multiple successive infections with *Ecc15* and determining the consequence of these repeated proliferative response for ISC numbers in the epithelium of the posterior midgut (Fig. 1 E–G). We found a significant, progressive decline of ISC numbers in animal exposed to 2 or more successive infections (Fig. 1F). This loss of ISCs was prevented when TOR activation was limited by over-expression of TSC1 and 2, and exacerbated when TOR was activated in the ISC lineage by knocking down TSC1 (Fig. 1G). When TOR activity was genetically induced in a repeated fashion by inducing the expression of a dsRNA against TSC1 3 times, ISC loss was also observed (Fig. 1H). Interestingly, the number of mitotic figures during the activated phase of the regenerative response was maintained even after 3 *Ecc15* exposures, indicating that under these conditions the remaining pool of ISCs was still large enough to fuel a vigorous regenerative response (Fig. S1A). However, there was a mild, but significant change in cell composition of the intestinal epithelium, with an elevated percentage of enteroendocrine cells at the expense of enterocytes (Fig. 1I).

At older ages, flies develop epithelial dysplasia in the intestine, characterized by chronic activation of ISCs (Biteau et al., 2010; Guo et al., 2014; Li et al., 2016; Wang et al., 2015). While this leads to a significant increase in mitotic figures even in unchallenged conditions, exposure to *Ecc15* still elevated mitotic figures in old flies (Fig. S1B). To test whether chronic TOR activity may contribute to ISC dysfunction in older animals, we asked whether marked lineages derived from individual ISCs (using the MARCM system, (Lee and Luo, 2001)) would be lost with age, and whether Rapamycin exposure was sufficient to rescue this phenotype (Fig. S1C). Indeed, we found that clone numbers declined in aging animals, and that this loss of functional ISCs was significantly slower when animals were exposed to Rapamycin (Fig. S1C).

The requirement for TOR activation to achieve a rapid regenerative response in the midgut thus also contributes to a progressive decline in ISC numbers and function. This observation has critical implications for our understanding of the loss of tissue homeostasis not only in flies, but also in aging vertebrates, and points to possible intervention strategies for the preservation of regenerative capacity in barrier epithelia. We thus sought to test whether a similar transient role for mTORC1 activity in regeneration, coupled to a loss of stem cells, is observed in a vertebrate barrier epithelium.

We chose the tracheal epithelium of the mouse as a system with high similarity to the fly intestinal epithelium. Basal Cells (BCs) in this epithelium are triggered to proliferate in

response to epithelial injury by SO2 exposure, and differentiation of early precursor cells is induced by BC-derived Delta-like signals (Fig. 2A). SO2 exposure results in the elimination of all differentiated cells of the epithelium, resulting in a monolayer of activated BCs at 1 day after exposure, which proliferate to restore epithelial cells (Fig. 2B and (Tata et al., 2013)). Further highlighting the similarity of epithelial regeneration in the fly intestine and the mouse trachea, we observed a transient induction of S6 phosphorylation (which we chose as a readout for mTORC1 pathway activity, as an antibody against p-4EBP is not reliable in paraffin sections) in basally located cells around 1 day after the SO2 exposure (Fig. 2B, D, S2A). This activation correlated with proliferative activation (as determined by Ki67 staining) of BCs. pS6/Ki67+ cells (the only remaining cells after the SO_2-induced ablation of differentiated tracheal epithelial cells) also expressed both the BC marker Keratin 5 (Krt5) and the differentiation marker Keratin 8 (Krt8), indicating that they constitute transient Basal Luminal Progenitor (BLP) cells (Fig. 2B, C, S2A–C). Between 3 and 8 days after the challenge, the structure of the epithelium was largely re-established, and S6 phosphorylation and Ki67 staining returned to basal levels (Fig. 2B, D). Furthermore, Krt5+ and Krt8+ cells segregated into Krt5+ BCs and Krt8+ differentiated cells (Fig. 2B, C, S2B). The transient induction of S6 phosphorylation was also observed in western blots of tracheal extracts (Fig. 2D, S2D), and correlated with a transient increase in size of Krt5+ cells (Fig. 2E).

Tracheal BC can be isolated and cultured in 3D cultures to generate ‘Tracheospheres’, organoids that consist of an epithelium with Trp63+/Krt5+ BCs, as well as ciliated and secretory differentiated cells. In growing spheres, sporadic activation of mTORC1 signaling (based on p-4EBP staining) can be observed in cells emerging from the basal layer, indicating that transient mTORC1 activity is part of the normal differentiation pathway in these organoids (Fig. 2F). Accordingly, inhibition of mTORC1 by Rapamycin treatment results in a decrease in Tracheosphere growth, thinning of the Tracheosphere epithelium, and accumulation of Trp63+ BCs (Fig. 2 G–I). We also observed a significant reduction in mitotic (pH3+) cell numbers, but not in apoptotic cells (detected using anti-cleaved Caspase 3 antibody) in Rapamycin-treated Tracheospheres (Fig. S2E, F). These observations suggest that mTORC1 signaling is critical for the establishment of a functional epithelium with differentiated cells, as well as for proliferation of BCs in the tracheal epithelium.

To ask whether, similar to the fly intestine, chronic or repeated activation of mTORC1 may negatively impact BC maintenance in mice, we performed repeated ablation of the epithelium by SO2 exposure, allowing the epithelium to recover for 2 weeks in between exposures (Fig. 3A). This regimen resulted in a significant loss of Trp63+ BCs in the epithelium, and this loss was dependent on mTORC1 signaling, as concurrent dietary supplementation with microencapsulated Rapamycin (42 ppm) (Flynn et al., 2013; Harrison et al., 2009; Miller et al., 2011; Wilkinson et al., 2012) resulted in a significant rescue of this phenotype (Fig. 3A). Repeated SO2 exposure further resulted in a mTORC1-dependent increase in secretory cells at the expense of BCs (Fig. S3A).

To further confirm the role of mTORC1 signaling in the loss of BCs, we genetically activated mTORC1 signaling in these cells. We used a Krt5::Cre^{ERT2} Tamoxifen-inducible driver to knock out TSC1 in BCs of young mice in combination with the Rosa26R-LacZ

transgene (Rock et al., 2009)(Fig. 3B). This resulted in a sustained increase of phospho-S6 in BCs (Fig. 3B, C, S3B), along with an increase in their size and activation of BC proliferation (Fig. 3C, S3B). Similar to fly ISCs, BCs of the tracheal epithelium may receive signals that activate mTORC1 in the absence of TSC1 during homeostatic renewal. While loss of TSC1 did not cause a significant change in the overall proportion of differentiated ciliated vs secretory cells under basal conditions (Fig 3C), epithelia with TSC1-deficient BCs accumulated Krt5+/Krt8+ cells after SO2 exposure, and these cells did not segregate into distinct Krt5+ and Krt8+ cell populations after the SO_2 treatment at the same rate as wild-type cells (Fig. 3D). Interestingly, loss of TSC1 in BCs caused epithelia to reacquire differentiated cells (both secretory and ciliated cells) at a faster rate than wild-type epithelia after SO2 exposure, suggesting that elevated mTORC1 activity may promote differentiation of BC-derived progenitors (Fig. S3B). We did not observe elevated levels of apoptosis in tracheal epithelia in which TSC1 was deleted from BCs (Fig. S3C).

These results indicate that, while mTORC1 activity in BCs contributes to activation of BCs, downregulation of mTORC1 activity is required for cells to return from an activated BLP state into a quiescent BC state.

TSC1-deficient BCs were observed at roughly the same rates as wild-type BCs in the tracheal epithelium up to 10 days after deleting TSC1, yet their numbers decline later on, resulting in a significant reduction of Krt5+ BCs at 28 days after Cre induction (Fig. 3E, F, S3D, E). To characterize the consequences of TSC1 loss in individual BC lineages, we used a Rosa26R::eYFP lineage tracer and reduced the numbers of Tmx injections from 4 to 3 (generating more isolated eYFP-marked BC lineages). 40 days after the Tamoxifen treatment, only 70% of TSC1-deficient clones contained a BC (based on Krt5 expression), while the rest contained only cells in a more differentiated state (Krt8+ cells). 100% of wild-type eYFP clones, instead, contained a stem cell (Fig. 3G, S3E). The decline in BC numbers in these lineages was primarily due to the increased differentiation of secretory cells (Fig. 3G, S3E). We observed similar phenotypes in tracheosphere cultures, where the number of Trp63+ BCs declined within 48 hours after induction of Cre (Fig. 3H, S3F).

We further tested whether other stem cell types may be subject to differentiation when mTORC1 is activated, and found that the muscle stem cell (MuSC) transcriptome acquires hallmarks of myogenic differentiation when TSC1 is knocked out, while differentiation markers are depleted when the mTORC1 component Raptor is knocked out (Fig. S3G, H). Accordingly, mTORC1 promotes the rapid expression of the myogenic differentiation marker, MyoG, in MuSCs following isolation. (Fig. S3I).

These results support the notion that sustained mTORC1 activation promotes the differentiation of mammalian tracheal and muscle stem cells, although further studies are needed to fully characterize the cellular response of stem cells to long-term mTORC1 activity.

Aging is accompanied by chronic activation of mTORC1 signaling in many tissues, and inhibition of TOR is sufficient to extend lifespan in a wide range of organisms (Bjedov et al., 2010; Garcia-Prat et al., 2016; Harrison et al., 2009; Markofski et al., 2015; Miller et al.,

2011; Wilkinson et al., 2012). Tracheal BC numbers decline with age (Wansleeben et al., 2014) through an unknown mechanism. Our results indicated that elevated or frequent mTORC1 activity, either during repeated regenerative episodes, or due to chronic activation of mTORC1, could cause this loss of BCs. To test this hypothesis, we first analyzed regeneration in the trachea of young and old mice, and found a sustained increase of BLP-like Krt5+/Krt8+ cells, accompanied by a mild (not statistically significant) reduction in proliferating cells (Ki67+) in response to SO2 exposure (Fig. 4, S4). These observations are consistent with mTORC1 gain-of-function phenotypes, and support the idea that elevated mTORC1 signaling impairs tracheal regeneration in old mice by increasing the probability of BCs entering or remaining in the BLP pre-differentiated state. Accordingly, we found elevated p-S6 levels in old BCs compared to BCs of young animals, both under homeostatic conditions and during regeneration (Fig. S4B, S5C). Furthermore, exposure to dietary Rapamycin was sufficient to promote return of Krt5+/Krt8+ BLPs into Krt5+ only BCs (Fig. 4A).

To test this hypothesis further, we asked whether inhibiting mTORC1 signaling chronically would be sufficient to maintain BC numbers in aging mice. Using dietary supplementation with microencapsulated rapamycin (14ppm) (Flynn et al., 2013; Harrison et al., 2009; Miller et al., 2011; Wilkinson et al., 2012), we tested the effects of long-term, chronic rapamycin treatment on BC maintenance and function. Female mice were treated either for 3 months (starting the rapamycin regimen at 9 or 15 months of age and sacrificed at 12 or 18 months, respectively), or for 12 months (starting at 12 months, sacrificed at 24 months; Fig. 5A). We observed increased proliferating cell numbers in basal conditions (Fig. S5A), restoration of the balance between secretory, ciliated and basal cells (Fig. S5B), reduced chronic mTORC1 activity in the epithelium (Fig. S5C), recovery of epithelial thickness in the trachea (Fig. 5B, S5D), as well as a significant increase in BC numbers in response to Rapamycin exposure in each of these conditions (Fig. 5C, D, S5B). Interestingly, tracheospheres derived from 18 months old animals exposed to Rapamycin for 3 months also showed a significant reduction in the accumulation of BLP-like Trp63+/Krt8+ cells. As observed in the tracheal epithelium of old mice, BCs from old mice generate tracheospheres with higher numbers of these BLPs than BCs from young mice. The fact that this phenotype was reduced in tracheospheres derived from Rapamycin-fed mice suggests that the beneficial effects of chronic mTORC1 inhibition is maintained in BCs *ex vivo* (Fig. 5E).

To test whether mTORC1 inhibition is sufficient to allay stem cell loss also in other tissues, we analyzed the consequences of mTORC1 signaling perturbation in aging muscle stem cells (MuSCs). Using a Pax7::Cre^{ER} driver associated with a Rosa26::EYFP lineage tracer, we observed a loss of MuSCs in aged mice. This loss of MuSC can either be amplified by knocking out TSC1, or rescued by knocking out Raptor in MuSCs (Fig. 5F, S5E).

Discussion

Our results suggest that the age-related loss of stem cells in various tissues is a consequence of the repeated activation of mTORC1 signaling during regenerative episodes (Fig. 6). The mechanism(s) of this activation remain to be established, but recent studies in fly imaginal discs point to a possible activation of mTORC1 downstream of CycD/cdk4 and/or E2F1

activation in the cell cycle (Kim et al., 2017; Romero-Pozuelo et al., 2017). In the fly intestine, the mouse trachea, and the mouse muscle, the need for mTORC1 activation to induce stem cell activity contrasts with the requirement for mTORC1 repression to maintain stem cell identity, and as a consequence, repeated episodes of regenerative pressure increase the probability of SC differentiation, resulting in the progressive loss of SCs. Critically, our findings also indicate that dietary supplementation with Rapamycin is sufficient to promote tracheal SC maintenance, and thus preserve regenerative capacity of airway epithelia. This is consistent with the fact that suppression of mTORC1 activity, through Rapamycin or genetic means, increases lifespan and slows the progression of other age-related phenotypes (Kennedy and Lamming, 2016).

Our results, and the observation that mTORC1 activation is required for the exit from quiescence of muscle stem cells, while sustained mTORC1 activation (e.g. through the loss of PTEN) also results in a decline of SC numbers in the hematopoietic system, the muscle, and the hair follicle, suggests that the tradeoff between mTORC1-mediated induction of SC proliferation and differentiation-induced loss is widely conserved (Castilho et al., 2009; Chen et al., 2011; Deng et al., 2015b; Easley et al., 2010; Kharas et al., 2010; Magri et al., 2011; Rodgers et al., 2014; Yilmaz et al., 2012; Yilmaz et al., 2006; Yue et al., 2016; Zhang et al., 2006). Based on our findings, it can thus be anticipated that long-term Rapamycin feeding will also promote SC maintenance in tissues other than the tracheal epithelium.

Our findings in fly ISCs, and the loss of TSC – deficient BCs and MuSCs, indicate that the preservation of BC numbers in the aging tracheal epithelium by Rapamycin feeding is a consequence of cell-autonomous repression of mTORC1 activity in these cells. It is possible, however, that Rapamycin elicits other local or systemic effects that promote stem cell maintenance. Non-autonomous effects of mTORC1 signaling on SC maintenance have been described for intestinal crypts of the mouse for example (Yilmaz et al., 2012), and additional studies will reveal whether such non-autonomous effects also apply to the mouse trachea or muscle.

Our data show that repeated transient activation of mTORC1 during regenerative episodes is sufficient to cause SC loss in both the fly intestine and the mouse tracheal epithelium. We propose that such repeated regenerative events along the lifespan of the animal results in increased probability of SC differentiation, thus causing SC loss over time. However, mTORC1 signaling activity may also be chronically elevated in SCs, as has been proposed for MuSCs (Garcia-Prat et al., 2016). Such chronic activation could contribute to the loss of SCs even in the absence of regenerative pressure. Whether conditions in which regenerative pressure is specifically reduced would result in improved SC maintenance in aging mice remains unclear. Identifying and studying such conditions would allow distinguishing whether repeated mTORC1 activation or chronic age-related elevation of mTORC1 activation are the primary drivers of SC loss in aging animals.

Our studies in the fly intestine have revealed that TOR activation is sufficient to promote ISC differentiation (Kapuria et al., 2012). In the mouse trachea, the transient formation of Krt5+/Krt8+ BLPs during regeneration, the correlation of their formation with mTORC1 activation, and their increased formation with elevated mTORC1 activity and in old animals,

are consistent with a similar differentiation-promoting role of mTORC1 in mammals. Accordingly, we find that TSC1-deficient BCs populate the SO2 depleted tracheal epithelium faster with differentiated ciliated and secretory cells than wild-type BCs. However, based on work in the hair follicle, it has also been proposed that mTORC1 may promote senescence of SCs (Castilho et al., 2009). We can thus not exclude that the effects of long-term Rapamycin exposure on BC maintenance are a consequence of reduced senescence or apoptosis rather than reduced differentiation. Studies that will explore the downstream mechanisms of mTORC1-mediated BC loss will likely resolve this question. In particular, the involvement of repressed autophagy or increased translation in mTORC1-mediated BC loss is going to provide critical insight. It is striking that the restoration of BC numbers in the old tracheal epithelium can be achieved even when Rapamycin is supplemented late in life (as late as 15 months of age). This may be explained by an increase in symmetric BC division when mTORC1 is inhibited and is consistent with a role for mTORC1 in promoting differentiation, as well as with the observation that mTORC1-deficient fly ISCs undergo symmetric divisions that result in small clusters of undifferentiated ISCs (Kapuria et al., 2012). However, these results may also indicate that de-differentiation of tracheal epithelial cells, which has been reported previously (Tata et al., 2013), may be increased in conditions of reduced mTORC1 activity. Importantly, this finding has important implications for the use of Rapamycin or Rapamycin analogues in clinical settings. Restoration of regenerative capacity of barrier epithelia by late-life Rapamycin administration emerges as a promising strategy for functional restoration in aging humans.

STAR METHODS

CONTACT FOR REAGENT AND RESOURCE SHARING

Further information and requests for resources and reagents should be directed to and will be fulfilled by the Lead Contact, Heinrich Jasper (jasperh@gene.com).

EXPERIMENTAL MODEL AND SUBJECT DETAILS

Drosophila stocks and culture—The following fly stocks were obtained from the Bloomington Drosophila Stock Center: w^{1118}, tub-Gal80^{ts}. UAS-TSC1^{RNAi} (Transformant ID 22252) was obtained from the Vienna *Drosophila* RNAi Center. The following lines were gifts from: hsFlp; tub-Gal4, UAS-GFP; FRT82A tubGal80, N. Perrimon; UAS-TSC1, TSC2, M. Tatar; FRT82A, by D. Drummond-Barbosa. Esg-Gal4, 2×UAS eYFP; Su(H)-GBE-Gal80, tubGal80ts (Wang et al., 2014).

Flies were cultured on yeast-molasses based food at 25°C, with 60% humidity and a 12 hour light/dark cycle.

For all experiments, flies were manipulated using a Drosophila anesthesia CO2 station.

Mouse strains and husbandry—All experiments were performed under the IACUC approved protocol # A10108 (tracheal epithelium study) or approved by the IACUC boards of the VA Palo Alto or USC (muscle study).

All mice were housed in a Specific Pathogen Free (SPF) facility, a HEPA filtered room and using a Tecniplast individually ventilated caging system/room. The room has controlled temperature (20–22°C), humidity (30–70%) and light (12 hour light-dark cycle). Unless otherwise indicated, mice were provided *ad libitum* access to a regular rodent chow diet, Teklad Global diet (2018, Harlan).

Wild-type C57BL/6J mice were ordered either from Jackson Laboratories or from the NIA (3month and 19month old mice for the aging experiments). KRT5-CreER^{T2} (Rock et al., 2009) were bred into Rosa26R-LacZ (Gt(Rosa)26Sor^{tm1Sor}) or Rosa26R-eYFP (Rock et al., 2009) reporter mice and TSC1^{tm1Djk}/J mice (stock # 005680, The Jackson Laboratory. This stock is originally in an SV129 background and was backcrossed 6 generations to C57BL/6 before crossing into the KRT5-CreER^{T2}; Rosa26R-LacZ line or KRT5CreERT2; Rosa26R-eYFP) to generate TSC1 conditional KO mice.

Pax7^{CreER} mice were provided by Dr. Charles Keller (OHSU). Rosa26^{EYFP}, TSC1^{flox}, and Rptr^{flox} animals were obtained from Jackson Labs. All experimental animals have a C57BL6-mix background, are male, and have the following genotypes: Pax7$^{CreER/+}$; Rosa26$^{EYFP/+}$ (Control), TSC1$^{flox/flox}$;Pax7$^{CreER/+}$;Rosa26$^{EYFP/+}$ (MuSC TSC1 cKO), Rptr1$^{flox/flox}$;Pax7$^{CreER/+}$;Rosa26$^{EYFP/+}$ (MuSC Rptr cKO).

Animals were genotyped by PCR of tail DNA.

For all experiments, mice were anesthetized by CO2 exposure followed by a terminal procedure (cervical dislocation or heart removal for tracheal studies).

METHOD DETAILS

Drosophila Target and MARCM clone induction—For TARGET experiments flies were raised at 18°C with 60% humidity and a 12 hour light-dark cycle, and shifted to the restrictive temperature (29°C) 3–5 days after eclosion. For clone induction (MARCM), 3–5 day old flies were heat shocked at 37°C for 30 minutes.

To induce pulses of TOR activity in the ISCs, flies expressing a RNAi against TSC1 specifically in the ISCs at a restrictive temperature (29°C) were kept at 18°C and shifted for 24h to 29°C. They went through three cycles of TOR activation (5 days at 18°C between each pulse).

Drosophila rapamycin Treatment—Flies were fed with normal fly food containing 200 μM Rapamycin starting from day 7 after clone induction. Flies were transferred into a fresh vial every 3–4 days.

Drosophila Ecc15 intestinal infection—To assess the ISC injury response, flies were orally infected by feeding *Ecc15* suspended in 5% sucrose as described previously (Deng et al., 2015a) or fed with 5% sucrose (control) and kept at 29°C. After 24 hours, flies were transferred back to clean vials with yeast-molasses food. Intestines were dissected at the given time-points.

Drosophila gut Immunostaining and Microscopy—Guts were dissected in phosphate-buffered saline (PBS) and fixed for 45min at room temperature in 100mM glutamic acid, 25mM KCl, 20mM $MgSO_4$, 4mM sodium phosphate, 1mM $MgCl_2$, and 4% formaldehyde. All subsequent washes (1h) and antibody incubations (4°C overnight) were performed in PBS, 0.5% bovine serum albumin and 0.1% Triton X-100.

Primary antibodies were: anti-phospho-4EBP1 (Thr37/46; rabbit, #2855, Cell Signaling; 1:200), anti-phospho-histone H3 (rabbit, #06-570, Millipore; 1:1000), anti-prospero (mouse, #MR1A, DSHB; 1:500), anti-pdm1 (rabbit, 1:500, kindly provided by Xiaohanh Yang at Zhejiang University). Secondary antibodies were Alexa Fluor conjugates (1:500, Life Technologies).

Confocal microscopy was performed on a Zeiss LSM 700 system. Multi-channel images were acquired by sequential scanning and further processed using FIJI (NIH ImageJ) and Adobe Photoshop. RGB composites of individual channels were created in FIJI and Photoshop. For display figures, channel brightness and contrast were adjusted for visibility, avoiding saturation or under-exposure, and figure panels were composed in Adobe Illustrator. Quantification of signal intensity was performed in FIJI, using unprocessed raw image files.

Only the middle posterior midgut region (region R4) was analyzed.

Mouse conditional KO and lineage tracing induction—In the trachea, to induce the recombination and TSC1 KO, adult mice (3 to 9 months old) were injected i.p. 4 times (or 3 for lineage tracing) every other day with 0.16 mg/g body weight Tamoxifen (Sigma) in 6% Ethanol and corn oil (ACH Food Companies). Mice injected with corn oil only were tested and did not present any sign of recombination. To reduce mortality due to bowel impaction observed in mice with these doses of Tamoxifen (Tmx), mice were fed with a complete nutritional gel diet, DietGel76A (ClearH20) 1 week prior and during the Tmx administration. Mice returned to regular rodent chow 3 days after the last Tmx injection. Mice health was monitored daily during the Tmx treatment.

For lineage tracing and clonal analysis using the Krt5-CreERT2 and the Rosa26R-eYFP reporter, mice received only 3 i.p. injections (one every other day) with 0.16 mg/g body weight Tmx.

In the muscle, to induce the recombination and TSC1 KO or Rptor KO, Tamoxifen (Sigma) was prepared in 7% EtOH and corn oil and administered to 3–4 months old mice in 5 doses of 5 mg/mouse every 2–3 days by intraperitoneal injection.

Mouse health was monitored daily during the time of the experiments.

Mouse Rapamycin treatment—For the treatments with Rapamycin, the microencapsulated Rapamycin was obtained by Rapamycin Holdings (http://rapamycinholdings.com/), then milled to the appropriate dose by Newco Distributors, Inc. (www.newcolab.com). Mice were fed with a micro-encapsulated rapamycin diet containing

a dose of 14 ppm (female mice) or 42 ppm (male mice) of Rapamycin *ad libitum* for the indicated time. The food was replaced every 3–4 days.

Mouse SO2 exposure—Adult male mice either young (3–4 month) or old (20 month) were exposed to 500ppm SO2 in air for 3 hours, using a flow rate of 3.3 L/min in a 20 L volume SO2 chamber (CH Technologies). In the case of the TSC1 KO mice, 4 to 6 months old animals were injected with Tmx as described above and exposed to SO2 at 10 days after the last Tmx injection. Mouse health was monitored over 6 hours after the end of the procedure.

For the repeated SO2 injury, adult male mice (3month) were exposed to SO2 as described above either for 1 exposure (1× SO2) or 3 exposures every other week for 6 weeks (3× SO2). Half of the mice for each group (1× and 3×) were fed Rapamycin food (42ppm), started immediately after the first SO2 exposure. All animals were sacrificed 2 weeks after the last SO2 exposure.

Mouse whole-mount immunohistochemistry—Tracheae were fixed over-night at 4°C in 4% paraformaldehyde. The next day, tissues were dehydrated and then paraffin embedded before sectioning (5μM). Primary antibodies were anti-Trp63 (mouse, 1:100 CM163B, Biocare Medical and mouse, 1:100 ab735, Abcam), anti-Krt5 (rabbit, 1:200 ab52635, Abcam), anti-Krt8 (rat, 1:100 TROMA-1-s, DSHB), anti-phospho-S6 (rabbit, 1:500 5364S, Cell Signaling), anti-Ki67 (rabbit, 1:200 ab15580, Abcam and mouse, 1:100 550609, BD Biosciences), anti-phospho-histone H3 (rabbit, 1:1000 06-570, Millipore), anti-GFP (chicken, 1:500, ab13970, Abcam), CCSP (goat, 1:100 sc-9772, Santa Cruz Biotechnology), AcTub (mouse, 1:5000 T7451, Sigma). Secondary antibodies were Alexa Fluor conjugates (1:500, Life Technologies). And processed with ProLong® Gold antifade reagent with DAPI (P36931, Invitrogen) for mounting.

For TUNEL staining, tracheal sections were processed following the *in situ* Cell Death Detection Kit (TMR Red, 12156792910, Roche) protocol from Sigma.

For lineage tracing using the Rosa26R::LacZ reporter, trachea were collected in PBS 2mM Mg2+. Followed by a 20min 2% paraformaldehyde fixation at room temperature. X-gal stained and over-night fixed with 4% paraformaldehyde at 4°C.

Confocal microscopy was performed on a Zeiss LSM 700 system. Image processing was done on FIJI (NIH Image J) using the same procedures described above under *Drosophila Gut Immunostaining and Microscopy.*

In situ analysis of MuSC number—Immediately after euthanasia, TA muscles were dissected, fixed in 0.5% PFA for 5 days at 4°C, and dehydrated in PBS 20% Sucrose overnight. After dehydration, TA muscles were embedded in O.C.T. (TissueTek) and frozen by emersion into liquid nitrogen cooled isopentane. After cryosectioning, 8μm sections were post-fixed in 4% PFA for 5 minutes and washed with PBS 0.3% Triton. To identify MuSCs, muscle sections were stained with Pax7 antibodies (DSHB) using the M.O.M. kit (Vector) according to the manufacturer's instructions. Following Pax7 staining, sections were blocked

with donkey serum and stained for GFP (Abcam, ab13970) and Laminin (Santa Cruz, sc-59854). To quantify MuSC number, sublaminar-YFP$^+$-Pax7$^+$ MuSCs were counted in a 20X field and normalized to the number of muscle fibers in the field, at least 10 fields were analyzed for each biological replicate.

Mouse tracheosphere culture—Tracheae were collected and incubated first in Dispase (BD Bioscience) diluted (1:2) in PBS for 30 min and followed by a DNase (0.4 units/uL) incubation for 5 min both at room temperature. The epithelium was carefully peeled off and transferred to a trypsin (0.1%) solution to dissociate the epithelial cells. Cells were resuspended in mouse tracheal epithelial cell (MTEC) media supplemented with FGF, EGF, FBS, Insulin, and Bovine pituitary extract (MTEC/Plus) (You et al., 2002) and counted to finally mix them 1:1 with growth factor-reduced Matrigel (BD Biosciences) and transferred (20 000 cells/insert) to a 24-well 0.4um Transwell insert (Falcon). 500uL of MTEC/Plus was added to the lower chamber and changed again the following day. Then media was changed every other day. Sphere culture were kept at 37°C with 5% CO2. Once the tracheospheres were formed (around 10 days), MTEC/SF was added to the lower chamber and changed every day.

Tracheosphere Rapamycin treatment and conditional KO—Epithelial cells from wild-type mice were used to induce tracheospheres formation. After 10 days, Rapamycin (final concentration 200nM, LC Laboratories) or EtOH 100% (control) was added to the MTEC/SF for 6 days. Medium was changed every day.

For TSC1 KO recombination in culture, epithelial cells from Krt5-Cre Rosa26R-LacZ with or without TSC1 fl/fl were used to induce spheres formation. After 9 days, 4-OH-Tmx (final concentration 300nM, Sigma) or EtOH 100% (control) was added to the MTEC/SF for 48h.

Then tracheospheres were fixed with 4% paraformaldehyde in PBS, stained and imaged as described above for whole trachea. Antibody used to detect cleaved Caspase-3 was rabbit anti-cleaved Casp3, 1:400 (#9661, Cell Signaling).

Western Blot—Individual tracheae were homogenized in RIPA buffer with Roche Proteinase Inhibitor Cocktail (1 tab/10mL RIPA), phosphatase inhibitors PI2 and PI3 (10uL each per 10mL RIPA), using a drill homogenizer, followed by protein quantification using Pierce BCA assay (ThermoFisher). Samples were resolved using 15% SDS-polyacrylamide gel electrophoresis, transferred to nitrocellulose membranes using semi-dry transfer, and probed with the following primary antibodies: anti-phospho-S6 (rabbit, 1:2000 5364S, Cell Signaling), anti-S6 (rabbit, 1:1000 22176, Cell Signaling), anti-α-Tubulin (mouse, 1:5000 T5168, Sigma). Antibodies were detected using horseradish peroxidase-conjugated secondary antibodies and the ECL detection system (Amersham).

QUANTIFICATION AND STATISTICAL ANALYSIS

All quantifications were done manually using FIJI (NIH ImageJ) software.

ISC and cell type quantifications in *Drosophila*

ISC and cell type quantifications were performed manually using the following markers: YFP (expressed under the control of esg::Gal4, Su(H)Gbe::Gal80 for ISCs), Prospero (for EEs) or Pdm1 (for ECs) in 3 squares of 100 μm sides per image. Three images were taken per fly (in the posterior midgut) and the average number of specific cell types per fly was calculated from these images. Averages were then used to calculate Mean and SEM for cell type numbers in a cohort of flies. N represents the number of animals.

pH3 positive nuclei quantifications in *Drosophila*

The number of pH3 positive nuclei per gut (in intestines stained against phospho-Histone H3) was manually quantified across the whole *Drosophila* midgut. N represents the number of animals.

ISCs size quantifications in *Drosophila*

ISCs size was measured manually in FIJI (ImageJ) software by determining the area of ISCs in representative micrographs. At least 10 ISCs were quantified per image, and 3 images per fly were used to calculate the average ISC size per fly. The Mean and SEM within a cohort of flies was then calculated. N represents the number of animals.

IHC p-4EBP1 quantification in *Drosophila*

Level of TOR activity was measured by quantifying the level of phospho-4EBP1 fluorescence (IHC staining) in individual ISCs normalized to nearby background. At least 10 ISCs were quantified in each image, and 3 images per fly were used to calculate the average intensity of p-4EBP1 in ISCs of each fly. Mean and SEM were calculated from these values for a cohort of animals. N represents the number of animals.

BCs and cell type quantifications in Mice

Quantification of BCs (IHC against Trp63) and other cell types (CC10 for secretory cells and AcTub for Ciliated cells), as well as of Krt5/Krt8 double positive cells was performed manually in in FIJI (NIH Image J). Six images were taken along the length of the trachea to calculate the average number of specific cells per mouse trachea. Mean and SEM were calculated using these values. N represents the number of animals.

For clone quantification, cells per clones were manually quantified as described above. All clones per frame were analyzed. At least 4 frames per trachea were analyzed to calculate the average per animal. Mean and SEM were calculated using these values. N represents the number of animals.

Ki67 positive nuclei quantifications in Mice

Ki67 positive nuclei were manually quantified along the whole trachea in IHC stained paraffin sections. Mean and SEM were calculated from these quantifications for a cohort of animals. N represents the number of animals.

BC size quantifications in Mice

BC size was measured manually with FIJI (ImageJ) software by determining the area of BCs in confocal micrographs. At least 10 BCs were quantified per image (and 6 images total per trachea) to calculate the average BC size per mouse trachea. Mean and SEM were calculated using these values. N represent the number of animals.

Tracheosphere size quantifications

Sphere size was measured manually with FIJI (ImageJ) software by determining the area of the sphere in micrographs. At least 30 spheres were quantified per image (and 6 images total per well) to calculate the average sphere size per well. Cells from individual animals were split into two wells to be treated with Rapamycin or control medium. N represents the number of animals.

p-S6 quantification in Mice

The level of phospho-S6 fluorescence was measured in BCs of IHC-stained tracheal sections using FIJI (NIH ImageJ) and normalized to nearby background. At least 10 BCs were quantified per image (and 6 images total per trachea) to calculate the average intensity of p-S6 in BCs of individual mice. Mean and SEM for a cohort of mice were calculated using these values. N represents the number of animals.

In western blots, band density was measured manually using FIJI (NIH ImageJ). Values for phospho-S6 were normalized to the levels of total S6 and α-Tubulin. N represents the number of animals.

Statistical analysis

Data representation and statistical analysis were performed using GraphPad Prism software. Power analysis was performed to determine the number of animals required to reach statistical significance for each experiment. Gaussian distribution of the data was assessed with a D'Agostino-Pearson Normality test. Pair-wise comparisons were performed with an ANOVA U-test. Multiple comparisons were performed with a One-Way ANOVA and Bonferroni's post-test.

All experiments were replicated independently 2–3 times.

Supplementary Material

Refer to Web version on PubMed Central for supplementary material.

Acknowledgments

This work was supported by NIA R01 AG047497 to H.J. and B.K.K. and NIH AG041764 to J.R. J.Q. is funded by R01 DK100342. We would like to thank Drs. Norbert Perrimon, Sarah Bray, Stephen X. Hou, Benjamin Ohlstein, Daniela Drummond Barbosa and Marc Tatar for flies, mouse tissue, and reagents, and Dr. David T. Madden, Matthew L. Donne, Dr. Jairo Barreta, Dritan Xhillari (CH Technologies) and Jay Palmer (ClearH20) for discussions, advice and technical support.

References

Amcheslavsky A, Ito N, Jiang J, Ip YT. Tuberous sclerosis complex and Myc coordinate the growth and division of Drosophila intestinal stem cells. J Cell Biol. 2011; 193:695–710. [PubMed: 21555458]

Ayyaz A, Jasper H. Intestinal inflammation and stem cell homeostasis in aging. Frontiers in cellular and infection microbiology. 2013; 3:98. [PubMed: 24380076]

Ayyaz A, Li H, Jasper H. Haemocytes control stem cell activity in the Drosophila intestine. Nat Cell Biol. 2015; 17:736–748. [PubMed: 26005834]

Biteau B, Hochmuth CE, Jasper H. JNK activity in somatic stem cells causes loss of tissue homeostasis in the aging Drosophila gut. Cell Stem Cell. 2008; 3:442–455. [PubMed: 18940735]

Biteau B, Hochmuth CE, Jasper H. Maintaining tissue homeostasis: dynamic control of somatic stem cell activity. Cell Stem Cell. 2011; 9:402–411. [PubMed: 22056138]

Biteau B, Karpac J, Supoyo S, DeGennaro M, Lehmann R, Jasper H. Lifespan extension by preserving proliferative homeostasis in Drosophila. PLoS Genet. 2010; 6:e1001159. [PubMed: 20976250]

Bjedov I, Toivonen JM, Kerr F, Slack C, Jacobson J, Foley A, Partridge L. Mechanisms of life span extension by rapamycin in the fruit fly Drosophila melanogaster. Cell Metab. 2010; 11:35–46. [PubMed: 20074526]

Castilho RM, Squarize CH, Chodosh LA, Williams BO, Gutkind JS. mTOR mediates Wnt-induced epidermal stem cell exhaustion and aging. Cell Stem Cell. 2009; 5:279–289. [PubMed: 19733540]

Chandel NS, Jasper H, Ho TT, Passegue E. Metabolic regulation of stem cell function in tissue homeostasis and organismal ageing. Nat Cell Biol. 2016; 18:823–832. [PubMed: 27428307]

Chen T, Shen L, Yu J, Wan H, Guo A, Chen J, Long Y, Zhao J, Pei G. Rapamycin and other longevity-promoting compounds enhance the generation of mouse induced pluripotent stem cells. Aging Cell. 2011; 10:908–911. [PubMed: 21615676]

Cheng LY, Bailey AP, Leevers SJ, Ragan TJ, Driscoll PC, Gould AP. Anaplastic lymphoma kinase spares organ growth during nutrient restriction in Drosophila. Cell. 2011; 146:435–447. [PubMed: 21816278]

Deng H, Gerencser AA, Jasper H. Signal integration by Ca regulates intestinal stem-cell activity. Nature. 2015a; 528:212–217. [PubMed: 26633624]

Deng Z, Lei X, Zhang X, Zhang H, Liu S, Chen Q, Hu H, Wang X, Ning L, Cao Y, et al. mTOR signaling promotes stem cell activation via counterbalancing BMP-mediated suppression during hair regeneration. J Mol Cell Biol. 2015b; 7:62–72. [PubMed: 25609845]

Easley, CAt, Ben-Yehudah, A., Redinger, CJ., Oliver, SL., Varum, ST., Eisinger, VM., Carlisle, DL., Donovan, PJ., Schatten, GP. mTOR-mediated activation of p70 S6K induces differentiation of pluripotent human embryonic stem cells. Cell Reprogram. 2010; 12:263–273. [PubMed: 20698768]

Flynn JM, O'Leary MN, Zambataro CA, Academia EC, Presley MP, Garrett BJ, Zykovich A, Mooney SD, Strong R, Rosen CJ, et al. Late life rapamycin treatment reverses age-related heart dysfunction. Aging Cell. 2013

Garcia-Prat L, Martinez-Vicente M, Perdiguero E, Ortet L, Rodriguez-Ubreva J, Rebollo E, Ruiz-Bonilla V, Gutarra S, Ballestar E, Serrano AL, et al. Autophagy maintains stemness by preventing senescence. Nature. 2016; 529:37–42. [PubMed: 26738589]

Guo L, Karpac J, Tran SL, Jasper H. PGRP-SC2 Promotes Gut Immune Homeostasis to Limit Commensal Dysbiosis and Extend Lifespan. Cell. 2014; 156:109–122. [PubMed: 24439372]

Harrison DE, Strong R, Sharp ZD, Nelson JF, Astle CM, Flurkey K, Nadon NL, Wilkinson JE, Frenkel K, Carter CS, et al. Rapamycin fed late in life extends lifespan in genetically heterogeneous mice. Nature. 2009; 460:392–395. [PubMed: 19587680]

Hsu HJ, Drummond-Barbosa D. Insulin levels control female germline stem cell maintenance via the niche in Drosophila. Proc Natl Acad Sci U S A. 2009; 106:1117–1121. [PubMed: 19136634]

Jasper H, Jones DL. Metabolic regulation of stem cell behavior and implications for aging. Cell Metab. 2010; 12:561–565. [PubMed: 21109189]

Jiang H, Patel PH, Kohlmaier A, Grenley MO, McEwen DG, Edgar BA. Cytokine/Jak/Stat signaling mediates regeneration and homeostasis in the Drosophila midgut. Cell. 2009; 137:1343–1355. [PubMed: 19563763]

Jones DL, Rando TA. Emerging models and paradigms for stem cell ageing. Nat Cell Biol. 2011; 13:506–512. [PubMed: 21540846]

Kapuria S, Karpac J, Biteau B, Hwangbo D, Jasper H. Notch-mediated suppression of TSC2 expression regulates cell differentiation in the Drosophila intestinal stem cell lineage. PLoS Genet. 2012; 8:e1003045. [PubMed: 23144631]

Kennedy BK, Lamming DW. The Mechanistic Target of Rapamycin: The Grand ConducTOR of Metabolism and Aging. Cell Metab. 2016; 23:990–1003. [PubMed: 27304501]

Kharas MG, Okabe R, Ganis JJ, Gozo M, Khandan T, Paktinat M, Gilliland DG, Gritsman K. Constitutively active AKT depletes hematopoietic stem cells and induces leukemia in mice. Blood. 2010; 115:1406–1415. [PubMed: 20008787]

Kim W, Jang YG, Yang J, Chung J. Spatial Activation of TORC1 Is Regulated by Hedgehog and E2F1 Signaling in the Drosophila Eye. Dev Cell. 2017; 42:363–375. e364. [PubMed: 28829944]

LaFever L, Drummond-Barbosa D. Direct control of germline stem cell division and cyst growth by neural insulin in Drosophila. Science. 2005; 309:1071–1073. [PubMed: 16099985]

LaFever L, Feoktistov A, Hsu HJ, Drummond-Barbosa D. Specific roles of Target of rapamycin in the control of stem cells and their progeny in the Drosophila ovary. Development. 2010; 137:2117–2126. [PubMed: 20504961]

Laplante M, Sabatini DM. mTOR signaling in growth control and disease. Cell. 2012; 149:274–293. [PubMed: 22500797]

Laplante M, Sabatini DM. Regulation of mTORC1 and its impact on gene expression at a glance. J Cell Sci. 2013; 126:1713–1719. [PubMed: 23641065]

Lee T, Luo L. Mosaic analysis with a repressible cell marker (MARCM) for Drosophila neural development. Trends Neurosci. 2001; 24:251–254. [PubMed: 11311363]

Li H, Jasper H. Gastrointestinal stem cells in health and disease: from flies to humans. Dis Model Mech. 2016; 9:487–499. [PubMed: 27112333]

Li H, Qi Y, Jasper H. Preventing Age-Related Decline of Gut Compartmentalization Limits Microbiota Dysbiosis and Extends Lifespan. Cell Host Microbe. 2016; 19:240–253. [PubMed: 26867182]

Magri L, Cambiaghi M, Cominelli M, Alfaro-Cervello C, Cursi M, Pala M, Bulfone A, Garcia-Verdugo JM, Leocani L, Minicucci F, et al. Sustained Activation of mTOR Pathway in Embryonic Neural Stem Cells Leads to Development of Tuberous Sclerosis Complex-Associated Lesions. Cell Stem Cell. 2011; 9:447–462. [PubMed: 22056141]

Markofski MM, Dickinson JM, Drummond MJ, Fry CS, Fujita S, Gundermann DM, Glynn EL, Jennings K, Paddon-Jones D, Reidy PT, et al. Effect of age on basal muscle protein synthesis and mTORC1 signaling in a large cohort of young and older men and women. Exp Gerontol. 2015; 65:1–7. [PubMed: 25735236]

McGuire SE, Le PT, Osborn AJ, Matsumoto K, Davis RL. Spatiotemporal rescue of memory dysfunction in Drosophila. Science. 2003; 302:1765–1768. [PubMed: 14657498]

McLeod CJ, Wang L, Wong C, Jones DL. Stem cell dynamics in response to nutrient availability. Curr Biol. 2010; 20:2100–2105. [PubMed: 21055942]

Micchelli CA, Perrimon N. Evidence that stem cells reside in the adult Drosophila midgut epithelium. Nature. 2006; 439:475–479. [PubMed: 16340959]

Miller RA, Harrison DE, Astle CM, Baur JA, Boyd AR, de Cabo R, Fernandez E, Flurkey K, Javors MA, Nelson JF, et al. Rapamycin, but not resveratrol or simvastatin, extends life span of genetically heterogeneous mice. J Gerontol A Biol Sci Med Sci. 2011; 66:191–201. [PubMed: 20974732]

O'Brien LE, Soliman SS, Li X, Bilder D. Altered modes of stem cell division drive adaptive intestinal growth. Cell. 2011; 147:603–614. [PubMed: 22036568]

Ohlstein B, Spradling A. The adult Drosophila posterior midgut is maintained by pluripotent stem cells. Nature. 2006; 439:470–474. [PubMed: 16340960]

Pardo-Saganta A, Law BM, Tata PR, Villoria J, Saez B, Mou H, Zhao R, Rajagopal J. Injury induces direct lineage segregation of functionally distinct airway basal stem/progenitor cell subpopulations. Cell Stem Cell. 2015; 16:184–197. [PubMed: 25658372]

Penney J, Tsurudome K, Liao EH, Elazzouzi F, Livingstone M, Gonzalez M, Sonenberg N, Haghighi AP. TOR is required for the retrograde regulation of synaptic homeostasis at the Drosophila neuromuscular junction. Neuron. 2012; 74:166–178. [PubMed: 22500638]

Quan Z, Sun P, Lin G, Xi R. TSC1/2 regulates intestinal stem cell maintenance and lineage differentiation via Rheb-TorC1-S6K but independent of nutrition status or Notch activation. J Cell Sci. 2013 in press.

Rock JR, Gao X, Xue Y, Randell SH, Kong YY, Hogan BL. Notch-dependent differentiation of adult airway basal stem cells. Cell Stem Cell. 2011; 8:639–648. [PubMed: 21624809]

Rock JR, Onaitis MW, Rawlins EL, Lu Y, Clark CP, Xue Y, Randell SH, Hogan BL. Basal cells as stem cells of the mouse trachea and human airway epithelium. Proc Natl Acad Sci U S A. 2009; 106:12771–12775. [PubMed: 19625615]

Rodgers JT, King KY, Brett JO, Cromie MJ, Charville GW, Maguire KK, Brunson C, Mastey N, Liu L, Tsai CR, et al. mTORC1 controls the adaptive transition of quiescent stem cells from G0 to G(Alert). Nature. 2014; 510:393–396. [PubMed: 24870234]

Romero-Pozuelo J, Demetriades C, Schroeder P, Teleman AA. CycD/Cdk4 and Discontinuities in Dpp Signaling Activate TORC1 in the Drosophila Wing Disc. Dev Cell. 2017; 42:376–387. e375. [PubMed: 28829945]

Sun P, Quan Z, Zhang B, Wu T, Xi R. TSC1/2 tumour suppressor complex maintains Drosophila germline stem cells by preventing differentiation. Development. 2010; 137:2461–2469. [PubMed: 20573703]

Tata PR, Mou H, Pardo-Saganta A, Zhao R, Prabhu M, Law BM, Vinarsky V, Cho JL, Breton S, Sahay A, et al. Dedifferentiation of committed epithelial cells into stem cells in vivo. Nature. 2013; 503:218–223. [PubMed: 24196716]

Vachias C, Fritsch C, Pouchin P, Bardot O, Mirouse V. Tight coordination of growth and differentiation between germline and soma provides robustness for drosophila egg development. Cell Rep. 2014; 9:531–541. [PubMed: 25373901]

Wang L, Ryoo HD, Qi Y, Jasper H. PERK Limits Drosophila Lifespan by Promoting Intestinal Stem Cell Proliferation in Response to ER Stress. PLoS Genet. 2015; 11:e1005220. [PubMed: 25945494]

Wang L, Zeng X, Ryoo HD, Jasper H. Integration of UPRER and oxidative stress signaling in the control of intestinal stem cell proliferation. PLoS Genet. 2014; 10:e1004568. [PubMed: 25166757]

Wansleeben C, Bowie E, Hotten DF, Yu YR, Hogan BL. Age-related changes in the cellular composition and epithelial organization of the mouse trachea. PLoS One. 2014; 9:e93496. [PubMed: 24675804]

Watson JK, Rulands S, Wilkinson AC, Wuidart A, Ousset M, Van Keymeulen A, Gottgens B, Blanpain C, Simons BD, Rawlins EL. Clonal Dynamics Reveal Two Distinct Populations of Basal Cells in Slow-Turnover Airway Epithelium. Cell Rep. 2015; 12:90–101. [PubMed: 26119728]

Wilkinson JE, Burmeister L, Brooks SV, Chan CC, Friedline S, Harrison DE, Hejtmancik JF, Nadon N, Strong R, Wood LK, et al. Rapamycin slows aging in mice. Aging Cell. 2012; 11:675–682. [PubMed: 22587563]

Yilmaz ÖH, Katajisto P, Lamming DW, Gültekin Y, Bauer-Rowe KE, Sengupta S, Birsoy K, Dursun A, Yilmaz VO, Selig M, et al. mTORC1 in the Paneth cell niche couples intestinal stem-cell function to calorie intake. Nature. 2012

Yilmaz OH, Valdez R, Theisen BK, Guo W, Ferguson DO, Wu H, Morrison SJ. Pten dependence distinguishes haematopoietic stem cells from leukaemia-initiating cells. Nature. 2006; 441:475–482. [PubMed: 16598206]

You Y, Richer EJ, Huang T, Brody SL. Growth and differentiation of mouse tracheal epithelial cells: selection of a proliferative population. Am J Physiol Lung Cell Mol Physiol. 2002; 283:L1315–1321. [PubMed: 12388377]

Yue F, Bi P, Wang C, Li J, Liu X, Kuang S. Conditional Loss of Pten in Myogenic Progenitors Leads to Postnatal Skeletal Muscle Hypertrophy but Age-Dependent Exhaustion of Satellite Cells. Cell Rep. 2016; 17:2340–2353. [PubMed: 27880908]

Zhang J, Grindley JC, Yin T, Jayasinghe S, He XC, Ross JT, Haug JS, Rupp D, Porter-Westpfahl KS, Wiedemann LM, et al. PTEN maintains haematopoietic stem cells and acts in lineage choice and leukaemia prevention. Nature. 2006; 441:518–522. [PubMed: 16633340]

Highlights

- Somatic stem cells transiently activate mTORC1 signaling during tissue regeneration
- Chronic mTORC1 activation leads to stem cell loss
- Repeated regenerative episodes result in mTORC1-dependent loss of SCs
- Long-term Rapamycin exposure limits age-related SC loss in the tracheal epithelium

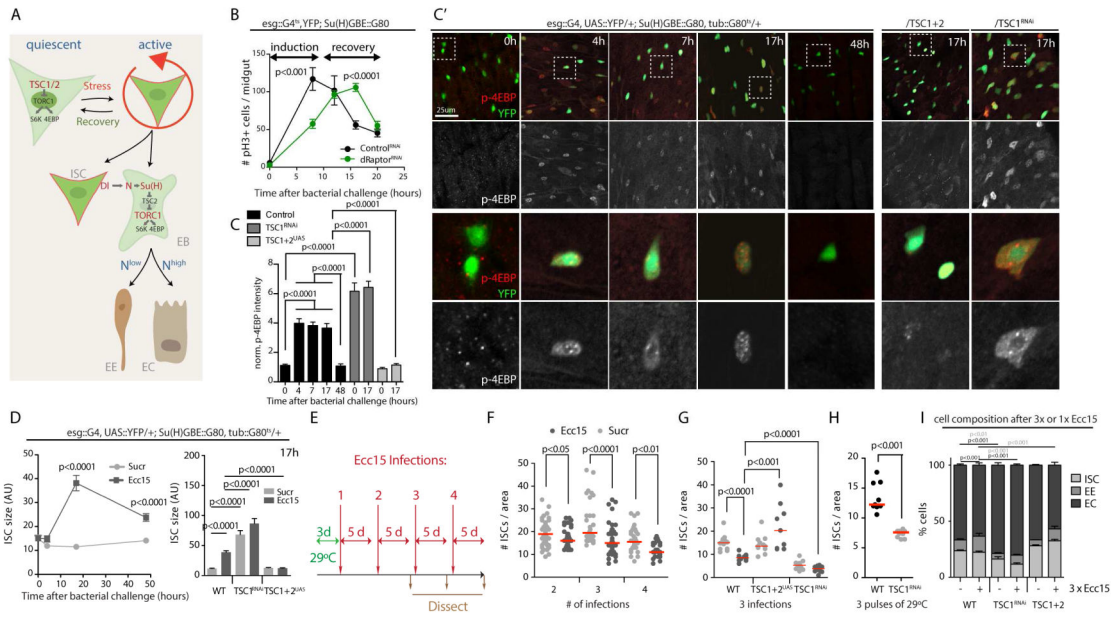

Figure 1. Repeated regenerative events lead to Tor-dependent ISC loss in *Drosophila*

A. Schematic representation of TOR-mediated differentiation in the ISC lineage in *Drosophila*. Quiescent ISCs exhibit low TOR activity due to the expression of high levels of TSC2. In response to tissue damage, ISCs divide asymmetrically and induce differentiation in their EB daughters by triggering Notch signaling. The level of Notch signaling activity determined differentiation into either ECs (high Notch) or EEs (low Notch). Notch activation results in TOR activation through the transcriptional repression of TSC2 in EBs. This activation of TOR is sufficient and required for differentiation into ECs.

B. Transient activation of ISC proliferation in response to *Erwinia Carotovora Carotovora* 15 (*Ecc15*) infection. Mitotic figures in whole intestines of wild type flies and flies expressing double-stranded RNA against dRaptor (dRaptor^{RNAi}), exposed to *Ecc15* for the indicated time-points are quantified using phosphorylated Histone H3 (pH3) as a marker. For each time-point, data points represent the average +/− SEM (n≥9) in a representative experiment. ANOVA U-test. Only female flies between 4 and 8 days of age were used for these experiments.

C, C′. Quantification of phospho-4EBP in ISCs (C) and confocal images of the middle posterior midgut (C′, region R4 is depicted) of flies expressing EYFP (green) in ISCs specifically (esg::Gal4, UAS::EYFP, Su(H)::Gal80) at indicated time-points after *Ecc15* infection. TOR activity is detected by immunohistochemistry against phospho-4EBP (p4EBP, red in upper panels, white in lower panels). Panels on the right show equivalent stainings at 17 hours after infection in flies over-expressing TSC1 and TSC2 (esg::Gal4, UAS::EYFP, Su(H)::Gal80/UAS::TSC1, UAS::TSC2) or a double-stranded RNA against TSC1 (TSC1^{RNAi}). Wild-type (WT) represents F1 of cross into the VDRC ID# 60000 control background. For each time-point and genotype n≥8 flies; representative images of one of at least three independent experiments are shown. Quantification of p-4EBP levels are mean fluorescence intensity in ISCs normalized to background. Bars represent the mean +/−

SEM (n>10). One-way ANOVA. Only female flies between 4 and 8 days of age were used for these experiments.

D. Analysis of ISC cell size in flies of the indicated genotypes exposed to *Ecc15* for the indicated timepoints (left panel). For each time-point and genotype, data points represent the mean +/− SEM (n≥8). On the right, analysis of the ISC cell size at 17h post Ecc15 infection, in wild type flies or in flies over-expressing TSC1 and 2 or double-stranded RNA against TSC1 in ISCs. Bars represent the mean +/− SEM (n>10). One-way ANOVA.

E. Protocol for repeated *Ecc15* infections. Flies were transferred to 29°C prior to the first *Ecc15* infection in order to induce the expression of transgenes, and then kept subsequently at 29°C.

F. Quantification of ISC numbers after repeated regenerative episodes. For each time-point and genotype, data points represent the number of ISCs per square (of 100×100μm) in separate guts. Red lines represent the median. ANOVA U-test.

G. Quantification of ISC numbers after three regenerative episodes in wild type flies or in flies over-expressing TSC1 and 2 or double-stranded RNA against TSC1 in ISCs. Data points represent the mean per animal, the red line indicate the median. ANOVA U-test.

H. Quantification of ISC numbers after three pulses of 29°C (24h per pulse, spaced by 5 days of 18°C) in wild type flies or flies over-expressing a double-stranded RNA against TSC1 in a temperature-inducible manner (tub::Gal80^{ts}). Data points represent the mean per animal, the red line indicates the median. ANOVA U-test.

I. Quantification of ISCs (YFP expression), EEs (prospero) and ECs (pdm1) present per square of 100 X 100μm in the middle posterior midgut of wild type flies, or flies over-expressing TSC1 and 2 or double-stranded RNA against TSC1 in ISCs after three regenerative episodes induced by *Ecc15* infection. Results are expressed as a percentage of total cells. Data represent the means +/− SEM (n>8). ANOVA U-test.

See also Figure S1.

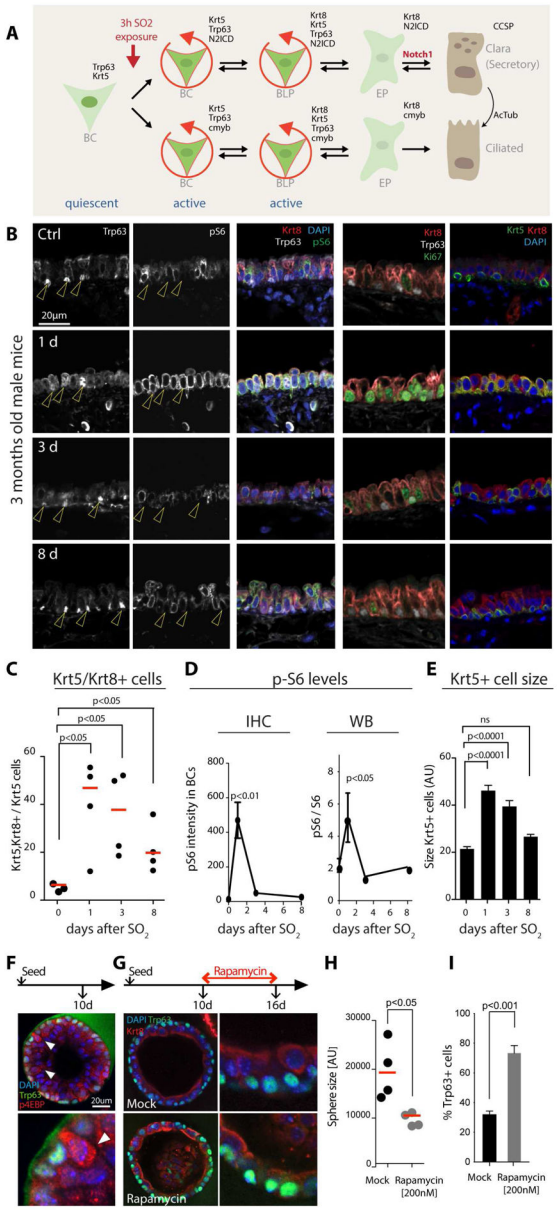

Figure 2. Tor signaling is induced in BCs upon regeneration and promotes differentiation

A. Schematic representation of the basal cell (BC) lineage in the tracheal epithelium. BCs (characterized by Krt5 and Trp63 expression) are mostly quiescent, but are activated upon epithelial damage, expressing either N2ICD (committed to the secretory cell lineage) or c-myb (ciliated cell lineage). These cells transition to basal luminal progenitors (BLPs), which express both Keratin5 (Krt5) and Keratin 8 (Krt8). Similar to *Drosophila* ISCs, BCs and BLPs express Notch ligands (Jag2 and Dll1) to activate Notch in early precursors (EPs) and induce their differentiation into Secretory Cells (CCSP expressing). Secretory Cells have the ability to divide and terminally differentiate into Ciliated Cells (acetylated Tubulin, AcTub). B. Confocal images of the proximal tracheal epithelium after SO_2 treatment. Mice were exposed to SO_2 for 3 hours to ablate differentiated cells of the epithelium. Trachea were

collected at 1, 3 and 8 days after SO_2 exposure. BC markers Trp63 and Krt5, the differentiated cell marker Krt8, and markers of stem cell activity (Ki67) and of Tor signaling activity (pS6) were detected by immunohistochemistry (IHC). For each time-point, panels show one representative epithelial section (SO_2 treated n=5 mice; n=3 controls). Arrowheads highlight Trp63+ BCs.

C. Quantification of the number of cells expressing both Krt5 and Krt8. For each time-point, each data point represents the fraction of Krt8+ cells among all Krt5+ cells for one trachea. Red lines represent the median. One-way ANOVA.

D. Quantification of the levels of pS6 in BCs during epithelial regeneration either by quantifying the IHC signal intensities or by western blot (WB on the whole trachea). Through IHC quantification pS6 intensity has been measured in BCs and normalized to the background. Through WB, pS6 levels have been normalized to the levels of total S6. For both graphs, data is represented as mean +/− SEM (n≥3). One-way ANOVA.

E. Analysis of BC size in the airway epithelium after SO_2 exposure. For each time-point data is represented as mean +/− SEM (SO_2 treated n=5; Controls n=3). One-way ANOVA.

F. Confocal images of a representative tracheosphere grown for 10 days. Spheres were stained for a BC marker (Trp63, green) and a marker of Tor activity (p4EBP, red). DAPI is shown in blue. Note high levels of p4EBP in cells emerging from the basal layer.

G. Confocal images of tracheospheres treated with Rapamycin (200nM) for 6 days. Spheres were stained for a BC marker (Trp63, green) and a differentiated cell marker (Krt8, red). DAPI is shown in blue. Panels show one representative out of n≥50 spheres. Note the loss of pseudostratification in the sphere epithelium after Rapamycin treatment.

H. Analysis of sphere size with or without Rapamycin treatment. Each data point represents the mean of sphere sizes from one trachea. Red lines represent the median of independent wells. ANOVA U-test.

I. Quantification of BC numbers (% Trp63+ cells of all cells) in spheres with or without Rapamycin treatment. Each bar represents the mean +/− SEM (n=6). ANOVA U-test.

See also Figure S2.

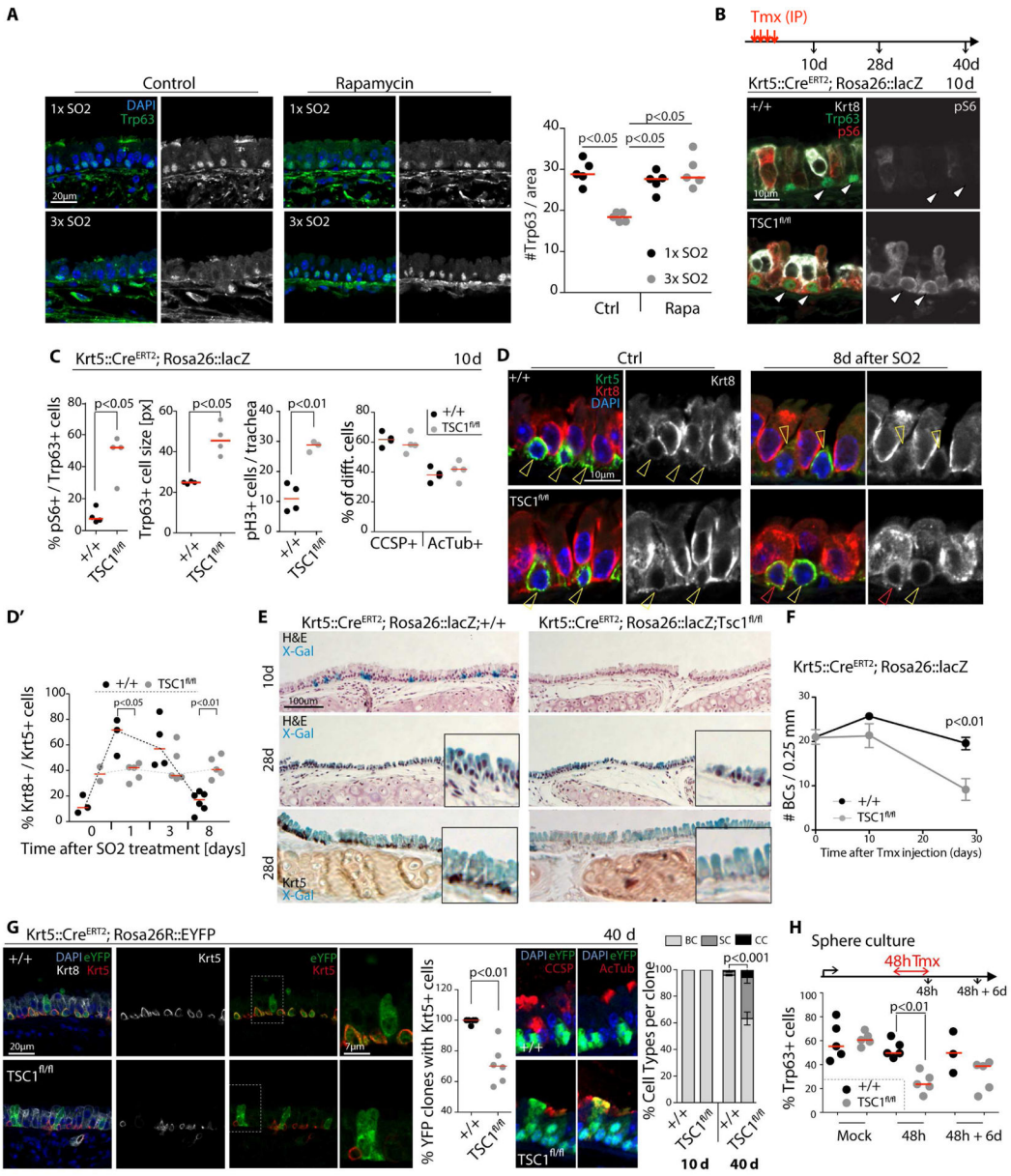

Figure 3. Loss of tracheal BCs after repeated regenerative episodes and after chronic activation of Tor signaling

A. Confocal images of an area of the tracheal epithelium after one SO2 (1× SO2) exposure or three SO_2 exposures (3× SO2, exposure performed every other week) in controls and Rapamycin treated mice, and corresponding quantification. Trp63 shown in green and grayscale, DAPI in blue. Each data point represents the mean for one trachea. Red lines represent the median. ANOVA U-test.

B. TSC1 deletor mice (Krt5::Cre^{ERT2}, Rosa26::lacZ/TSC1$^{fl/fl}$) or controls (Krt5::Cre^{ERT2}, Rosa26::lacZ/+) were injected 3 or 4 times intra-peritoneally (IP) with Tamoxifen (one injection every other day) to induce TSC1 deletion specifically in BCs. Animals were euthanized and trachea collected at 10 days, 28 days (4 injections of Tamoxifen) and 40 days (3 injections of Tamoxifen) post Tamoxifen injection, respectively.

Confocal images of the central region of the airway epithelium. IHC was performed to detect Trp63 (green), Krt8 (white in left panels), p-S6 (red in left, white in right panels), as well as phospho-Histone H3 to detect mitotic cells (not shown). Images show a representative epithelium of n≥4 samples analyzed.

C. The percent of Trp63+ cells expressing high levels of pS6, the size of Trp63+ cells (in pixels), the number of pH3+ cells in the whole trachea and the proportion of secretory (CCSP+) and ciliated (AcTub) cells are represented. Each data point represents the mean for one trachea. Red lines represent the median. ANOVA U-test.

D. Confocal images of an area of the tracheal epithelium and quantifications of Krt5+/Krt8+ double-positive BLPs at the indicated timepoints after SO_2 exposure in controls (Krt5::Cre^{ERT2}, Rosa26::lacZ/+) or TSC1 deletor mice (Krt5::Cre^{ERT2}, Rosa26::lacZ/TSC1$^{fl/fl}$). IHC detecting Krt5 (green) and Krt8 (red and white). One representative epithelium (n≥5 for 8 day sample is shown). Yellow arrows indicate Krt5 only, while red arrows indicate Krt5/Krt8 double positive cells.

D′. Corresponding quantifications. Each data point represents the mean for one trachea. Red lines represent the median. One-way ANOVA.

E. Brightfield images of X-Gal and Hematoxylin/Eosin stained tracheal epithelia of control (Krt5::Cre^{ERT2}, Rosa26::lacZ/+) or TSC1 deletor mice (Krt5::Cre^{ERT2}, Rosa26::lacZ/TSC1$^{fl/fl}$) at indicated timepoints after Tamoxifen injection. X-Gal and IHC against Krt5 (in black) shown in lower panels. Pictures show one representative stained epithelium (n≥4).

F. Quantification of BC numbers in confocal sections at indicated times after the last Tamoxifen injection. Each data point represents the mean per trachea +/− SEM (n≥4). One-way ANOVA.

G. Confocal images of an area of the tracheal epithelium at 40 days after Tamoxifen treatment of controls (Krt5::Cre^{ERT2}, Rosa26::eYFP/+) or TSC1 deletor mice (Krt5::Cre^{ERT2}, Rosa26::eYFP/TSC1$^{fl/fl}$), and the corresponding quantifications (%) of eYFP clones containing BCs (Krt5+) and the different cell types present in the eYFP clones (BCs, Secretory and Ciliated cells). Each data point (quantification of clones containing BCs) represents the mean for one trachea. Red lines represent the median (n≥5). Bars (cell type analysis) represent the mean +/− SEM (n>4). ANOVA U-test.

H. Quantification of Trp63+ cells (BCs) in tracheospheres derived from control (Krt5::Cre^{ERT2}, Rosa26::lacZ/+) or TSC1 deletor mice (Krt5::Cre^{ERT2}, Rosa26::lacZ/TSC1$^{fl/fl}$). Spheres were grown for 9 days, then exposed to Tamoxifen for 2 days. Each data point represents the mean for one sphere. Red lines represent the median. One-way ANOVA. See also Figure S3.

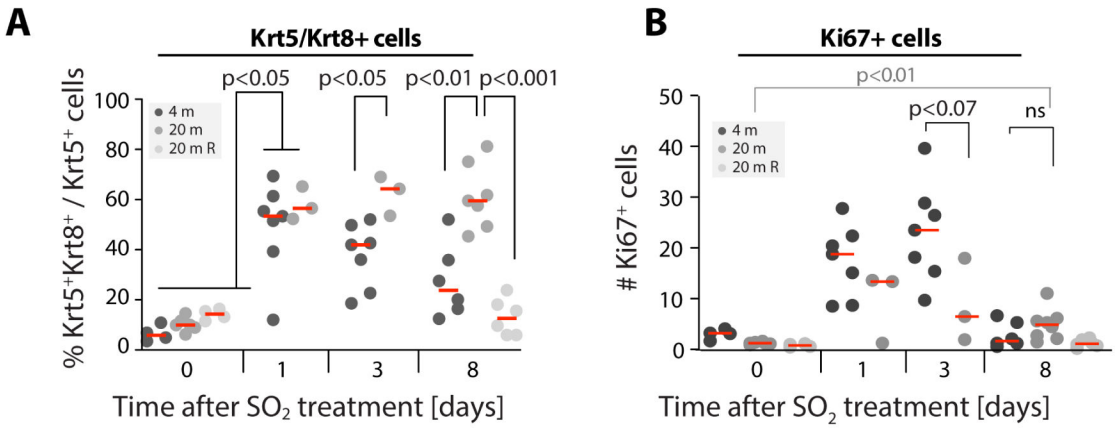

Figure 4. Accumulation of BLPs in the regenerating old tracheal epithelium

A. Quantifications of Krt5+/Krt8+ cells in young (4 months old), old (20 months old) and old Rapamycin treated (3 month of Rapamycin, 42ppm) epithelia after SO_2 exposure. Each data point represents the mean for one trachea. Red lines represent the median. One-way ANOVA.

B. Quantifications of Ki67+ cells in young (4 months old), old (20 months old) and old Rapamycin treated (3 month of Rapamycin 42ppm) epithelia after SO_2 exposure. Each data point represents the mean for one trachea. Red lines represent the median. One-way ANOVA.

See also Figure S4.

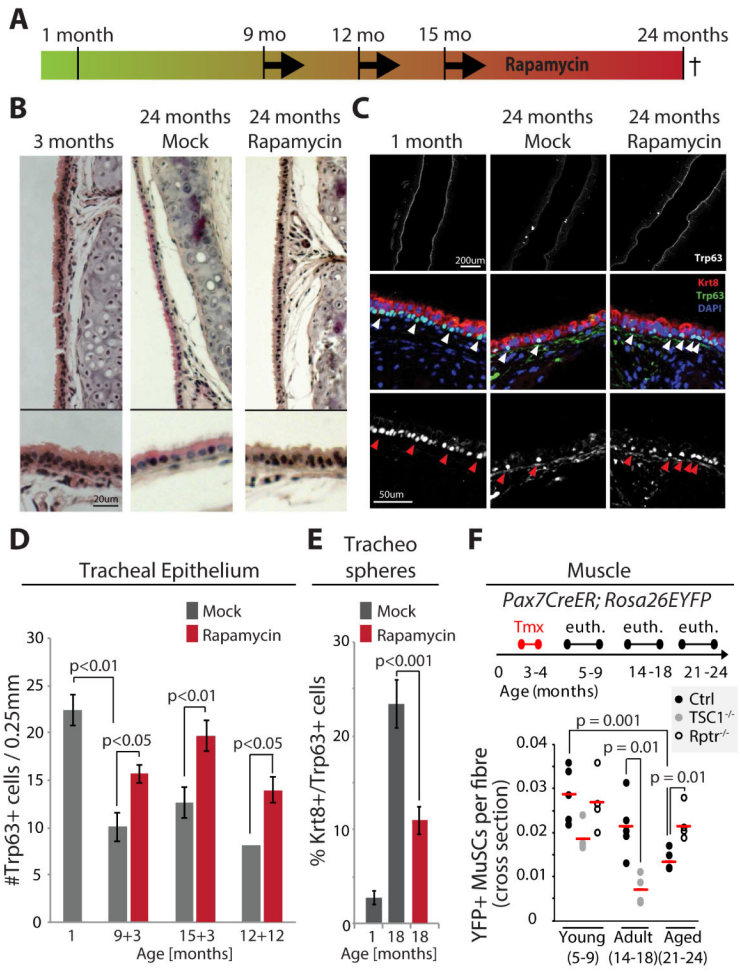

Figure 5. Chronic repression of Tor signaling rescues the loss of BCs observed in old mice

A. Schematic of Rapamycin exposure for chronic repression of Tor. Mice were fed Rapamycin for 3 months starting either at 9 or 15 month of age, or for 12 months starting at 12 month of age.

B. Bright field images of H&E stained airway epithelium of young (3 months old), old (24 months old) and old Rapamycin-treated (24 months old exposed to Rapamycin food for 12 months) mice.

C. Confocal images of an area of the airway epithelium of young (3 months old), old (24 months old) and old Rapamycin-treated (24 months old exposed to Rapamycin food for 12 months) mice. IHC against Trp63 (white and green) and Krt8 (red). Upper panels are low magnification (5×) showing most of the trachea, lower panels are high magnification (40×) showing a section of the tracheal epithelium.

D. Quantification of BCs (Trp63+) in the airway epithelium of either young or old mice with or without Rapamycin treatment. Genotypes of all mice were C57BL/6J with the exception of the mice analyzed at 9+3 months, which were FVB/N. Averages and SEM are shown, Student's Ttest (1 month old: n=4; 9+3 months: n=4 Control and n=3 Rapamycin; 12+12 months: n=2 Control and n=6 Rapamycin).

E. Quantification of Krt8+/Trp63+ double-positive cells in tracheospheres derived from 1 month or 18 month old mice that were fed Rapamycin containing or control food for 3 months (15+3). Averages and SEM are shown, Student's Ttest. n=5 mice at 1 month old, N= 10 mice for 18 months old samples. 6–10 Spheres per mouse were quantified.
F. Schematic outline of the timecourse of Tmx treatment and euthanizing of mice at young, adult, and aged timepoints in Control mice ($Pax7^{CreER/+}$; $Rosa26^{EYFP/+}$), MuSCs TSC1 cKO mice ($TSC1^{flox/flox}$;$Pax7^{CreER/+}$;$Rosa26^{EYFP/+}$) and MuSC Rptr cKO mice ($Rptr1^{flox/flox}$;$Pax7^{CreER/+}$;$Rosa26^{EYFP/+}$). YFP^{+}-$Pax7^{+}$ MuSC were quantified by IHC staining of tibial anterior (TA) muscle cross-sections and normalized to the number of muscle fibers in a field. Each data point represents the mean for one animal (n≥4).
See also Figure S5.

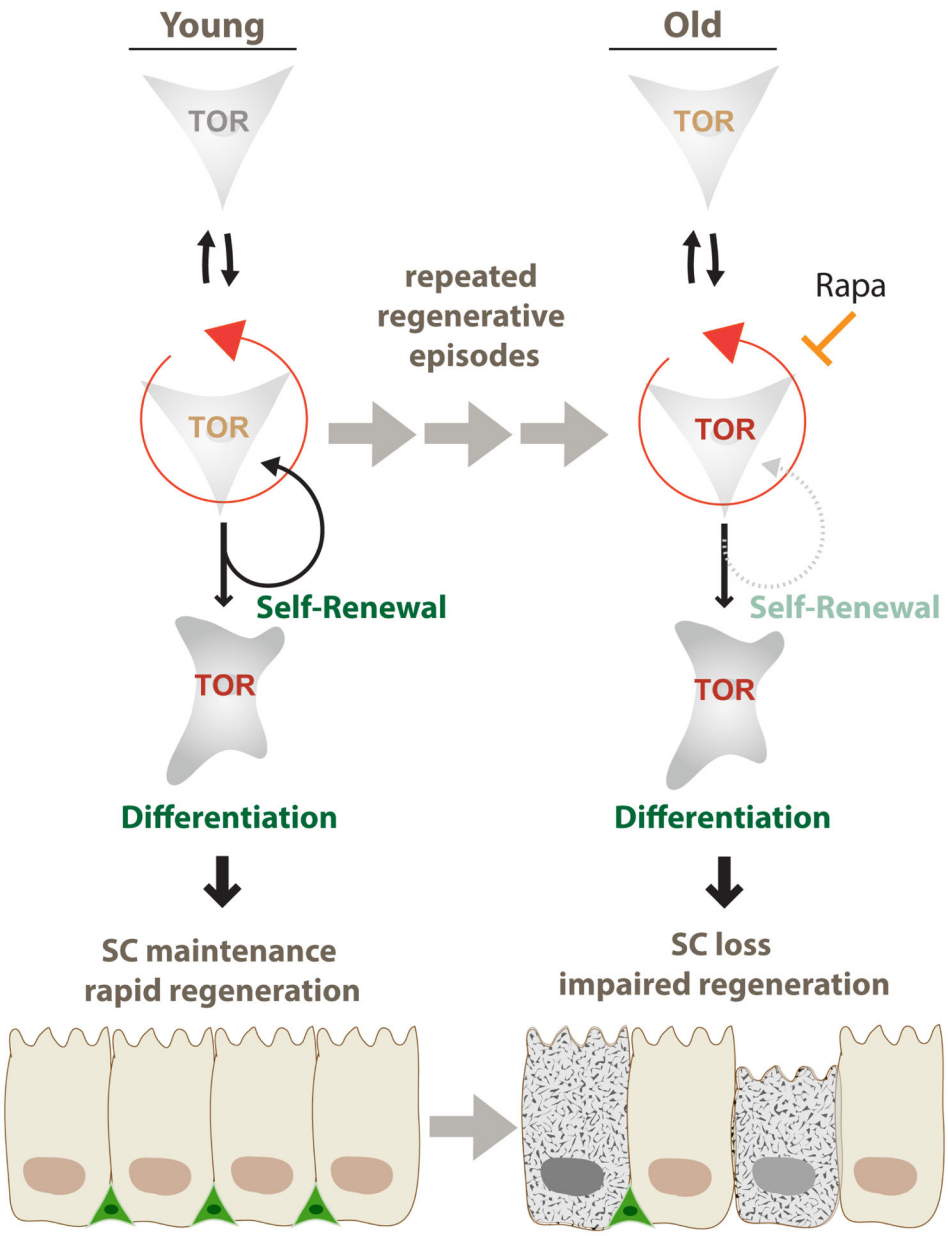

Figure 6. Model for the role of repeated transient mTORC1 activation events resulting in progressive BC loss in aging epithelia

Upon regeneration, stem cells transiently activate mTORC1 signaling in order to rapidly repair the tissue. Stochastically, some stem cells fail to down regulate mTORC1 activity after regeneration and are driven to differentiation, resulting in loss of stem cells. Repeated regenerative episodes during the life-time of an animal thus results in a loss of BCs that can be reversed by chronic supplementation with Rapamycin.